Modelling an air handling unit, building and occupant, regarding energy, moisture and frost protection

Marius Daugela

Master thesis in Energy-efficient and Environmental Buildings
Faculty of Engineering | Lund University

Lund University

Lund University. with eight faculties and a number of research centers and specialized institutes. is the largest establishment for research and higher education in Scandinavia. The main part of the University is situated in the small city of Lund which has about 112 000 inhabitants. A number of departments for research and education are. however. located in Malmö. Lund University was founded in 1666 and has today a total staff of 6 000 employees and 47 000 students attending 280 degree programs and 2 300 subject courses offered by 63 departments.

Master's Program in Energy-efficient and Environmental Building Design

This international program provides knowledge. skills and competencies within the area of energy-efficient and environmental building design in cold climates. The goal is to train highly skilled professionals. who will significantly contribute to and influence the design. building or renovation of energy-efficient buildings. taking into consideration the architecture and environment. the inhabitants' behavior and needs. their health and comfort as well as the overall economy.

The degree project is the final part of the master program leading to a Master of Science (120 credits) in Energy-efficient and Environmental Buildings.

Examiner: Birgitta Nordquist (Division of Building Services)

Supervisor: Dennis Johansson (Division of Building Services)

Keywords: Heat exchanger, Frost, Condensation

Publication Year: 2022

Abstract

Residential homes in Europe use 26.6% of Europe's total energy consumption (eea.europa.eu, 2015). A simple and efficient solution to lower energy costs used to be to recycle exhaust air for warming the incoming air. However, this system is not commonly used anymore because the recycled air has to be filtered to meet the regulation levels and because filters cannot trap particles. They are in general regarded as unhygienic. Nowadays the most common energy recovery system in Sweden is heat exchangers. (Abel & Elmroth, 2007)

Objectives of this paper are firstly, to analyze selected indoor and outdoor climate conditions, secondly, to propose a reasonable simulation model, thirdly, to analyze risk of frost formation and discuss different frost protection strategies.

Using psychometrics. ASHRAE heat exchanger calculation. condensation and frost calculation methods, heat plate exchanger and enthalpy wheel were simulated in Jupiter Notebook. Calculations were done using two methods.

The first method was to take the heat exchanger as a whole. using efficiency as a static number for simplification purposes. The heat exchanger was assumed to be a dimensionless unit. Using this type of approach. the performances of the crossflow plate heat exchanger and enthalpy wheel were simulated for every hour of the year.

The second method was to simulate the crossflow plate heat exchanger in more detail. a two-dimensional model was subdivided into small squares. Subdivision of the heat exchanger module allowed to simulate the exchanger in greater detail to see where the condensation and frost happened and if it blocked exhaust airstreams.

The calculation of the heat exchanger module was done in the following steps: The first step was to divide the U value according to the subdivision of the heat exchanger. Then, estimated flow rates were subdivided accordingly. Then, each subdivision was considered as a ''small'' independent exchanger, while the whole module was considered as a chain of many small exchangers. Putting the values into matrixes made it possible to analyze data for every hour of the year.

It was concluded that the risk of frost in heat exchangers was highest in Kiruna and Ostersund due low outdoor air temperatures during the winter, however heat recovery systems in Copenhagen and Gothenburg still had a risk of frost formation even though these cities had relatively warm weather conditions. The study showed that moisture supply was unevenly occurring within building's apartments, suggesting that the moisture load in a heat exchanger could be reduced by having less, but bigger heat exchangers that gather exhaust air streams from several apartments at once.

Out of several simulation models that were created during the study, the detailed model that takes condensation effect into consideration, was proven to be worthy to be used in further investigations, due to results that more accurately represent real word conditions.

Risk of frost formation became significantly lower in every city when heat recovery ventilation was changed into energy recovery ventilation. Because heat was not the only type of energy that could be recovered, changing heat recovery ventilation system into energy recovery ventilation system enabled latent as well as heat energy recovery, making this system more efficient. Even though heat recovery ventilation was simulated only with the simplified model, it is safe to assume that it will still be effective in reality. Although bypass strategies were effective at eliminating the risk of frost in heat recovery units, they were not as efficient from energy perspective. The more air is by-passed the cross-flow plate heat exchanger, the fewer opportunities there are to recover energy from exhaust air, which leads to lower supply air temperatures and higher energy need for heating a living space.

Table of content

Terminology / Notation

(Choose one of the headline alternatives.) A possible list of terms. abbreviations and variable names with brief explanations may be placed after the table of contents. or at the end of the report. but is not required. Note that although a term is explained in the list of terms. it should also be explained in the chapter text where it is used the first time.

U	*U-value. W/m²°C*
ε_s	*Sensible effectiveness %*
t_{sae}	*Supply air entering dry-bulb temperature.* $°C$
t_{sal}	*Supply air leaving dry-bulb temperature.* $°C$
t_{eae}	*Exhaust air entering dry-bulb temperature.* $°C$
t_{eal}	*Exhaust air leaving dry-bulb temperature.* $°C$
c_{pe}	*Exhaust moist air specific heat at constant pressure.* $kJ/kg \cdot K$
c_{ps}	*Supply moist air specific heat at constant pressure.* $kJ/kg \cdot K$
m_e	*Exhaust dry air mass flow rate.* kg/s
p_{ws}	*Saturation pressure. Pa*
T	*Absolute temperature. K*
w_{sal}	*Supply air leaving humidity ratio.* kg_w/kg_{da}
w_{sae}	*Supply air entering humidity ratio.* kg_w/kg_{da}
w_{eae}	*Exhaust air entering humidity ratio.* kg_w/kg_{da}
w_{eal}	*Exhaust air leaving humidity ratio.* kg_w/kg_{da}
p_{tot}	*Total atmospheric pressure. Pa*
p_w	*Partial pressure of water vapor. Pa*
ϕ	*Relative humidity. %*
q_s	*Actual energy transfer*
ρ_s	*Density of dry supply air.* kg_{da}/m^3
ρ_e	*Density of dry exhaust air.* kg_{da}/m^3
Q_s	*Volume flow rate of supply air.* m^3/s
Q_e	*Volume flow rate of exhaust air.* m^3/s
ε_L	*Latent effectiveness %*
m_s	*Supply dry air mass flow rate.* kg/s
C_r	*Heat capacity ratio*
UA	*Overall heat transfer coefficient. W°C*
NTU	*Number of transfer units*

1 Introduction

Residential homes in Europe use 26.6% of Europe's total energy consumption (eea.europa.eu, 2015). A simple and efficient solution to lower energy costs used to be to recycle exhaust air for warming the incoming air.

Figure 1 Building leaking energy

However, this system is not commonly used anymore because the recycled air has to be filtered to meet the regulation levels and because filters cannot trap particles. They are in general regarded as unhygienic. Nowadays the most common energy recovery system in Sweden is heat exchangers. (Abel & Elmrofth, 2007)

Heat exchangers can be categorized as heat recovery ventilation (figure 2) and energy recovery ventilation (figure 3). In a heat recovery ventilation heat exchanger, heat flows over the surface where the heat exchange occurs. In a energy recovery ventilation heat exchanger, the exchange happens through a heat transferring mass that is cooled by the incoming air and heated by the exhaust air.

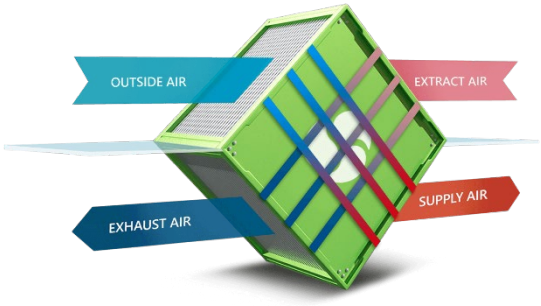

Figure 2 Heat recovery ventilation (HRV)

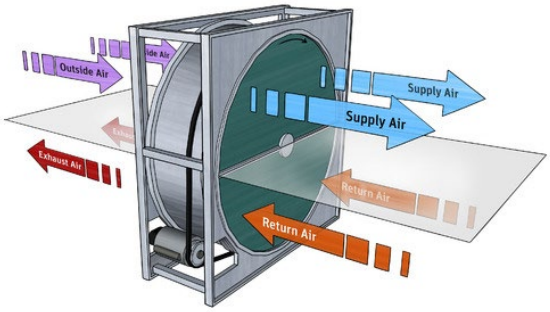

Figure 3 Energy recovery ventilation (ERV)

Heat exchangers have the greatest potential of saving energy in cold climates, where incoming and exhaust air temperature difference is the greatest. However, the lower the outdoor temperature, the greater the risk of frost formation. When the outdoor temperature is low enough to bring the temperature of the exhaust air bellow its saturation point, latent energy of the exhaust air stream is released, heat is transferred to the supply air stream and condensation forms on the walls of the heat exchanger. Condensation is a welcome side effect as it increases

the total amount of energy that can be transferred (figure 4) (INCROPERA, DEWITT, BERGMAN, & LAVINE, 2007).If the temperature of the heat exchanger drops below zero, condensation can turn into frost (figure 5) which can cause various problems to the heat

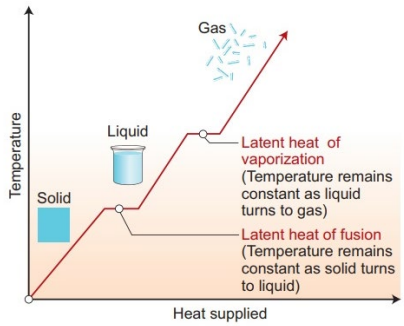

Figure 4 latent heat of vaporization and fusion

exchanger. Accumulated frost shuts off heat exchanger pathways and reduces exhaust air flow. In extreme scenarios, the heat exchanger must be turned off for long periods of time for ice to be melted. Because water expands while freezing, ice deforms the heat exchanger, (figure 6)

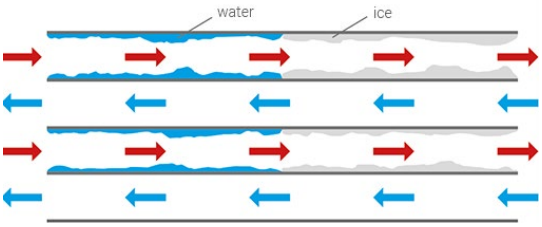

Figure 5 Frost formation

lowering the efficiency and introducing leakages and an increased pressure drop over the whole system. (Rafatinasr, 2016).

Condensation and frost can be closely related to occupant behavior because the more moister is supplied indoors, the more condensation and frost occurs in the heat exchanger. The perfect system should be able to take advantage of condensation while preventing condensate turning into frost.

Figure 6 Frost formation damages integral structure of materials

In practically used soft wares such as “VIP Energy”. “Designbuilder” or “IDA ICE”, there still is not a good way to model energy use, moisture flows, and different defrosting strategies for

different types of heat exchangers in air handling units. With a badly working defrosting strategy, a lot of heat recovery could be lost and other problems in low energy houses could emerge. This is one of the remaining big problems with ventilation systems in dwellings in some Nordic climates, that needs to be understood better in order to solve it.

This thesis focuses primarily on heat recovery ventilation systems that are more popular due to their lower price and high efficiency. Energy recovery systems are analyzed in less detail. The main difference between the two systems is that while heat recovery ventilation system recovers only heat energy recovery ventilation system can also recover latent energy.

1.1 Overall aim and objectives

Due to lack of a good way to model energy use, moister flows, and different defrosting strategies, a lot of heat recovery can be lost. This project seeks to model an air handling unit, a building and occupant behavior, regarding energy, moisture, and frost protection. The analysis will be carried out using secondary data from a case study analysis on occupant impact on air humidity, and by developing a detailed simulation model of a heat exchanger, which should help determine how different types of heat exchangers perform under different Nordic weather conditions, and what type of freezing protection systems perform the best.

Objectives of this paper are firstly, to analyze selected indoor and outdoor climate conditions, secondly, to propose a reasonable simulation model, thirdly, to analyze risk of frost formation and discuss different frost protection strategies.

1.2 Scope

This study is limited to Nordic weather conditions alone and measurements of moisture production were taken from one building which is assumed to represent the general moisture production in apartment buildings. The study focused on cross flow heat plate exchangers and enthalpy wheel heat exchanger. It also focused on risk factors of frost and few frost strategies. leaving out transmission losses and energy consumption of fans, motors, and buildings' heating systems. The study analyzed different heat exchangers, disregarding their prices.

In reality, the heat exchanger would stop working after frost formation. In the paper the frost is considered continuously removed so that the heat exchanger could theoretically continue working.

1.3 Contributions

The work was caried out by Marius Daugela with the consultation of Dennis Johansson. Examiner was Birgitta Nordquist.

2 Methodology / Model

2.1 Outdoor climate conditions

Outdoor conditions were extracted from Energy Plus weather format files (National Renewable Energy Laboratory, 2020). Files contained: atmospheric pressure and dry bulb and relative humidity (RH) for every hour of a year. Cities of interest are Kiruna, Stockholm, Gothenburg, Copenhagen and Ostersund Figure 7, which shows Mean temperature of January in Nordic countries.

Since freezing in exhaust air stream can only happen when temperature drops below 0°C. the number of hours when it can happen are of interest. Using the equation (1) and having prescribed efficiency, one can estimate how many hours the heat exchanger was at risk of frost formation.

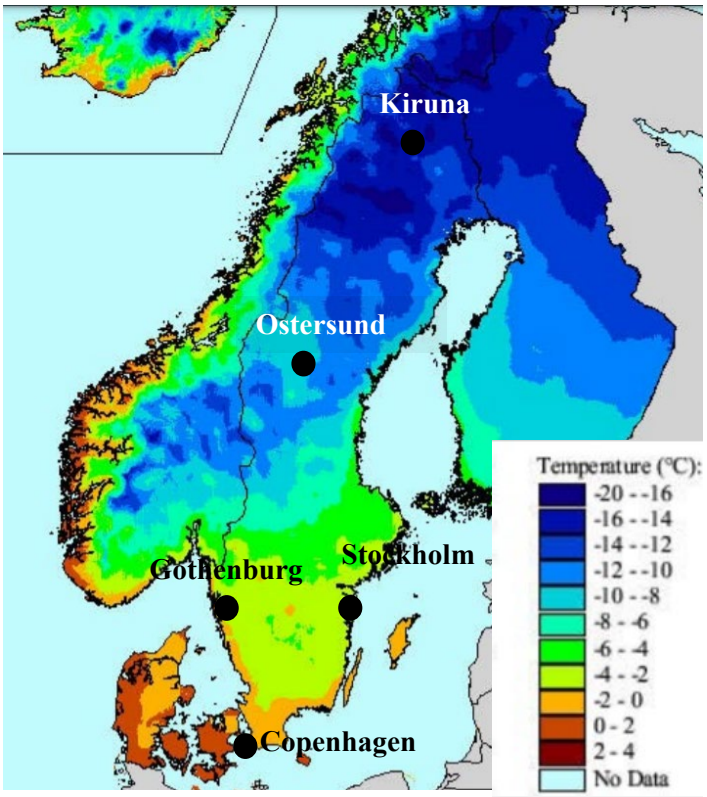

Figure 7 Cities of interest for further analysis Temperatures during January

$$t_{outdoor} = \frac{t_{eal} - t_{eae}}{\varepsilon_s \frac{C_{min}}{C_e}} + t_{eae} \,.°C \quad (1)$$

Where:
ε_s = sensible effectiveness %

t_{sae} = supply air entering dry-bulb temperature. $°C$

t_{sal} = supply air leaving dry-bulb temperature. $°C$

t_{eae} = exhaust air entering dry-bulb temperature. $°C$

t_{eal} = exhaust air leaving dry-bulb temperature. $°C$

$C_{min} = smaller\ of\ c_{ps} \cdot m_s\ and\ c_{pe} \cdot m_e . kJ/s \cdot K$

c_{pe} = exhaust moist air specific heat at constant pressure. $kJ/kg \cdot K$

c_{ps} = supply moist air specific heat at constant pressure. $kJ/kg \cdot K$

m_e = exhoust dry air mass flow rate. kg/s

2.2 Indoor climate conditions and psychrometric calculations

Indoor climate conditions were taken from the study "Hygrotermiska Förhållanden I Inomhusluften" (Bagge & Johansson, 2015). For further analysis only the data from building in Karlstad was used. The building has 36 apartments ranging in size from 60 m^2 to 92 m^2. averaging on 74.75 m^2. Each apartment had an exhaust ventilation system. Total exhaust air flow was 0.35 l/s/m^2 and was available in channels in the attic, where measuring equipment was placed. The temperature and relative humidity were measured in the exhaust duct from each apartment.

The temperature and relative humidity sensors had a specified accuracy of ± 1.5% relative humidity (RH) for RH between 0% and 80%, and ± 2% RH for RH between 80% and 100%. The temperature had a specified accuracy of ± 0.25°C for temperatures lower than 0°C, and ± 0.1°C for temperatures around 20°C. The interval between the measurements was 6 min.

Moisture supply was calculated using psychrometric calculations, based on measured temperatures and relative humidity. The difference between the vapor content, measured in each apartment's exhaust air and in the outdoor air, defines the apartment's moisture supply. The measurements were aggregated on hourly level for faster processing in future simulations. This means that a specific moisture supply from an individual apartment for each hour during the year was used in the calculations.
To perform heat exchanger analysis, number of moist air properties are required.
Water vapor saturation pressure values were obtained using following formulas (Hyland & Wexler, 1983b).

The saturation pressure over ice from temperatures ranging of -100 to 0°C is given by

$$ln\ p_{ws} = \frac{C_1}{T} + C_2 + C_3 T + C_4 T^2 + C_5 T^3 + C_6 T^4 + C_7 lnT,\ Pa \quad (2)$$

where

C1 = -5674.5359
C2 = 6.3925247
C3 = -0.009677843
C4 = 0.00000062215701
C5 = 0.0000000020747825
C6 = -0.0000000000009484024
C7 = 4.1635019

The saturation pressure over ice from temperatures ranging of 0 to 200°C is given by

$$ln\ p_{ws} = \frac{C_8}{T} + C_9 + C_{10}T + C_{11}T^2 + C_{11}T^2 + C_{12}T^3 + C_{12}lnT, Pa \quad (3)$$

where
C8 = -5800.2206
C9 = 1.3914993
C10 = -0.048640239
C11 = 0.000041764768
C12 = -0.000000014452093
C13 = 6.5459673
$p_{ws} =$ saturation pressure, Pa

$T =$ absolute temperature , K $= ℃ + 273.15$, K

The coefficients of equations (1) and (2) were derived from Hyland -Wexler equations and taken from ASHRAE fundaments (American Society of Heating, Refrigerating and Air-Conditioning Engineers, 2009).

Moist air was considered a mixture of independent perfect gases (dry air and water vapor). Humidity ratio W was expressed:

$$W = 0.621\,945\ \frac{p_w}{p - p_w}, kg_w/kg_{da} \quad (4)$$

From relative humidity:

$$W = \frac{0.621945\ \phi p_s}{p_{tot} - \phi p_s}, kg_w/kg_{da} \quad (5)$$

Where
$p =$ total preasurre, Pa
$p_w =$ partial preasure of water vapor, Pa
ϕ-relative humidity, %

Specific volume v of moist air mixture was expressed in terms of a unit mass of dray air:

$$v = 0.287\,\frac{042(t+273.15)(1+1.607\,858W)}{p}\ , m^3/kg_{da} \quad (6)$$

To find out humidity ratio indoors, the formula was derived to include moisture supply from the occupants:

$$W = \left(\frac{w_{se}}{sv}\right) + \left(\frac{msp}{3600}/Q_e\right) \cdot 0.833, kg_w/kg_{da} \quad (7)$$

2.3 Simulation models

Visual representation of all the simulation models that were carried out in the study figure 8.

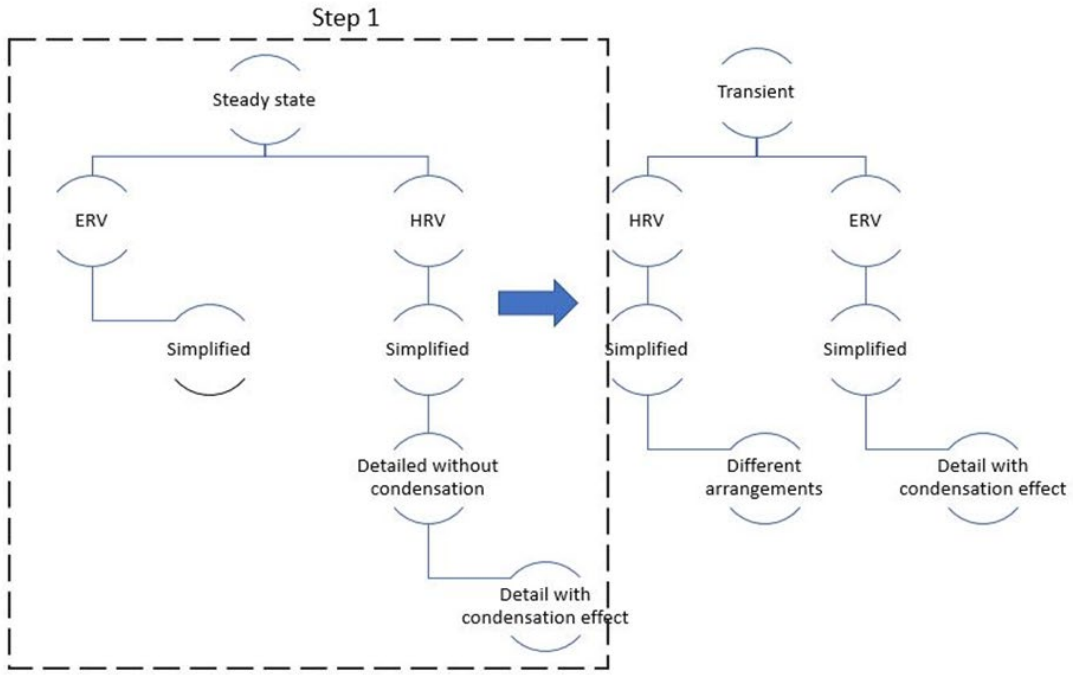

Figure 8 Process flow chart for developing simulation models

2.4 Simplified heat exchanger simulation

The simulation was carried out on heat recovery ventilation (HRV) and energy recovery ventilation (ERV). The HRV and ERV systems facilitate energy transfer from exhaust room temperature air to incoming supply outdoor temperature air during winter and opposite during the summer, via metal plate surface.

Temperature efficiency facilitates only sensible heat transfer. The energy efficiency facilitates total, sensible and latent energy transfer.

HRV/ERV efficiency depends on its geometry, arrangement of air streams and material, According to ASHRAE (American Society of Heating, Refrigerating and Air-Conditioning Engineers, Inc., 2012), counter flow exchanges, which is a subset of HRV, have theoretical maximum temperature efficiency approaching 100%, but the actual temperature efficiency is

typically lower. Typical cross flow unit's effectiveness is 50 to 70%. Typical enthalpy wheel, which is a subset of ERV, has a theoretical temperature efficiency of 80%. However, energy efficiency consists of moisture and sensible heat efficiency that are not necessarily the same.

In real life conditions efficiency is not constant, it changes over time depending on the temperature difference, the amount of condensation and heat capacity rate. The thermal capacity is a product of mas flow rate and specific heat. In the simplified simulation, latent and sensible efficiency is a constant. In most cases it is more than enough for an engineer to use an average efficiency to select the HRV/ERV. Manufacturers provide measurements of average efficiency for balanced flow conditions. In practice, due to construction and size limitations, designs that use crossflow are typically favored. That is why crossflow exchangers were chosen to be the main subject of this project.

2.4.1 Steady state sensible heat recovery ventilation

Steady state analysis was performed based on theoretical worst-case scenarios - highest moisture supply under negative temperatures, ASHRAE Standard 84 defines efficiency of a heat recovery system:

$$\varepsilon_s = \frac{Actual\ transfer\ of\ energy}{Maximum\ posible\ transfer\ between\ airstreams}, \% \quad (8)$$

$$\text{Actual energy trasfer} = q_s = Q_s\rho_s c_{ps}(t_{sae} - t_{sal}) = Q_e\rho_e c_{pe}(t_{eae} - t_{eal}), \quad (9)$$

$$Maximum\ posible\ transfer\ between\ airstreams = C_{min}(t_{ee} - t_{se}) \quad (10)$$

$$C_{min} = smaller\ of\ Q_s\rho_s c_{ps}\ and\ Q_e\rho_e c_{pe} \quad (11)$$

Assuming no water vapor condensation in the HRV, leaving supply air temperature is:

$$t_{sal} = t_{sae} - \varepsilon_s \frac{C_{min}}{Q_s\rho_s c_{ps}}(t_{sae} - t_{eae}), ℃ \quad (12)$$

Leaving supply air temperature is:

$$t_{eal} = t_{eae} - \varepsilon_s \frac{C_{min}}{Q_e\rho_e c_{pe}}(t_{sae} - t_{eae}), ℃ \quad (13)$$

Where

ε_s = sensible effectiveness, %

t_{sae} = supply air entering dry-bulb temperature, $°C$

t_{sal} = supply air leaving dry-bulb temperature, $°C$

t_{eae} = exhaust air entering dry-bulb temperature, $°C$

t_{eal} = exhaust air leaving dry-bulb temperature, $°C$

ρ_s = density of dry supply air, kg_{da}/m^3

ρ_e = density of dry exhaust air, kg_{da}/m^3

Q_s = volume flow rate of supply air, $m^3\ /s$

Q_e = volume flow rate of exhaust air, $m^3\ /s$

c_{ps} = supply moist air specific heat at constant pressure, $kJ/kg \cdot K$

c_{pe} = exhaust moist air specific heat at constant pressure, $kJ/kg \cdot K$

2.4.2 Steady state total energy recovery ventilation

Steady state analysis was performed based on theoretical worst-case scenarios - highest moisture supply under negative temperatures.

ASHRAE Standard 84 defines efficiency of a heat recovery system:

$$\varepsilon_L = \frac{Actual\ transfer\ of\ moisture}{Maximum\ posible\ transfer\ between\ airstreams} \quad (14)$$

$$Total\ transfer\ of\ energy = q_s = Q_e\rho_e c_{pe}(t_{eae} - t_{eal}) + \ m_e h_{fg}(w_{eae} - w_{eal}) \quad (15)$$

$$Maximum\ \ posible\ transfer\ between\ airstreams = C_{min}(t_{ee} - t_{se}),\ kJ/kg \quad (16)$$

$$C_{min} = \ smaller\ of\ Q_s\rho_s c_{ps}\ and\ Q_e\rho_e c_{pe}\ , kJ/kg \cdot K \quad (17)$$

Assuming there was no water vapor condensation in the HRV, leaving supply air water content is:

Leaving supply air water content is:

$$w_{sal} = \ w_{sae} - \varepsilon_L \frac{m_{w,min}}{m_s}(w_{sae} - \ w_{eae}),\ \mathrm{kg_w}\ /\mathrm{kg_{da}} \quad (18)$$

$$w_{eal} = \ w_{sae} + \varepsilon_L \frac{m_{w,min}}{m_s}(w_{sae} - \ w_{eae}),\ \mathrm{kg_w}\ /\mathrm{kg_{da}} \quad (19)$$

Where

ε_L = lathen efficiency, %

ρ_s = density of dry supply air, kg/m^3

ρ_e = density of dry exhaust air, kg/m^3

Q_s = volume flow rate of supply air, m^3/s

Q_e = volume flow rate of exhaust air, m^3/s

m_s = supply dry air mass flow rate, kg/s

2.4.3 Transient state sensible heat and total energy recovery ventilation

Using measurements (relative humidity outdoors and indoors, temperature indoors and outdoors) for each individual apartment for every hour of the year, from the study "Hygrotermiska förhållanden i inomhusluften" (Bagge & Johansson, 2015) and statistical weather conditions in different parts of Sweden, calculations were coded in a python model, using formulas previously discussed in the chapters ''2.3.1 Steady state heat recovery ventilation'' and "2.3.2 Steady state total energy recovery ventilation'', and iterated over every hour of the year.

2.4.4 Simulating different heat exchangers arrangements

The moisture supply is different in every apartment, due to different amount and behaviors of residents. Redirecting exhaust air from more than one apartment into one heat exchanger could reduce moisture load on the heat exchanger.

To analyze the risk of frost, different heat exchanger set-ups were simulated: one for the whole building; one for 18 apartments (randomly grouped using a Python script); one for nine apartments (randomly grouped using a Python script); one for four apartments (randomly grouped using a Python script); one for each apartment, The fewer heat exchangers were used, the bigger they needed to be, which was accounted for in the Python script. Bigger units got more moisture, but the air flow was higher. To access the risk of frost formation, hours of condensation under negative exhaust air leaving temperatures were counted for every apartment.

2.5 Detailed heat exchanger simulation

Because the simplified model did not take into account condensation and freezing in different areas of the heat exchanger, due to not uniform temperatures across the heat exchanger, the detailed model was developed. The detailed model took into account the temperature stratification across the heat exchanger and condensation affect.

2.5.1 Steady state detailed model

To perform a detailed analysis the heat exchanger 2d cross section was subdivided into small squares and the calculation was performed on each individual square level Figure 9. Consequently, the more in detail the cross area was subdivided, the more accurate the results would be.

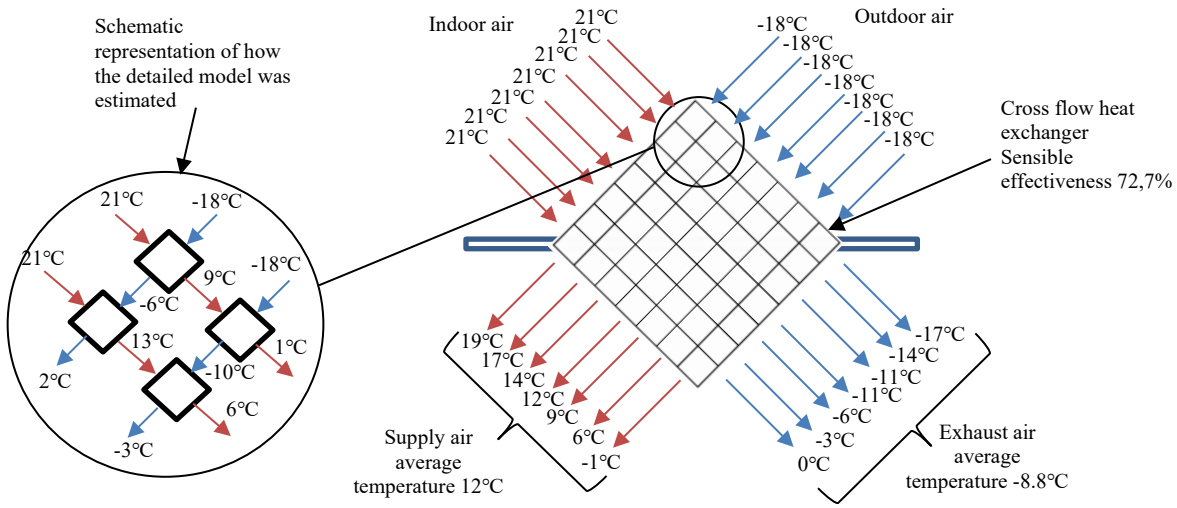

Figure 9 Cross flow 72.7% effectiveness heat exchanger schematic representation. The heat exchanger subdivided 7x7 granularity

The rate of energy transfer depended on operating conditions, geometry of the heat exchanger, heat transfer surface area and thermal conductivity of the walls separating the streams.

During the analysis two modes of energy transfer were considered. The first mode is the energy transfer driven by the dry bulb temperature difference between cross-streams. Second mode was latent heat transfer, when water vapor condensed on the walls in the heat exchanger and released latent heat to another air stream as sensible heat.

2.5.1.1 Energy transfer due to dry bulb temperature difference

In practice, efficiency is not constant, it changes over time depending on heat capacity rate. The thermal capacity is a product of mas flow rate and specific heat.

The simplified model used efficiency only, the model was dimensionless. To perform calculations on individual 2d square level, the dimensions of the heat exchanger were introduced. To define the dimensions, UA-value of the heat exchanger was used.

Size and thermal conductivity of the heat exchanger (UA-value) were taken into account, using effective – NTU (ε-NTU) method. Knowing prescribed effectiveness of the heat exchanger and the heat capacity ratio equation (20) one could use the Figure (10) (Dewitt, Incropera, Bergman, & Lavine, 2007) to see the NTU value for the prescribed efficiency. Once the NTU value was established, a heat exchanger could be chosen to match the required surface area and the U value (UA – value) equation (21).

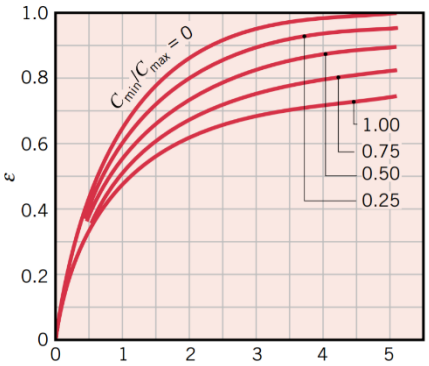

Figure 10 Effectiveness of cross flow heat exchanger with both fluids unmixed equation (22)

$$C_r = \frac{(mc_p)_{min}}{(mc_p)_{max}} \tag{20}$$

$$UA = NTU(mc_p)_{min} \tag{21}$$

Temperatures of the incoming air streams and the NTU value effected minimum heat capacity and heat capacity ratio. Having prescribed overall heat transfer coefficient (UA) one can estimate how NTU equation (23) and efficiency equation (22) variated under different inlet conditions.

$$\varepsilon = 1 - \exp\left\{\left(\frac{1}{C_r}\right) NTU^{-0.22}[\exp(-C_r \cdot NTU^{0.78}) - 1]\right\}, \% \tag{22}$$

$$NTU = \frac{UA}{(mc_p)_{min}} \tag{23}$$

c_p = moist air specific heat at constant pressure, $kJ/kg \cdot K$

m = dry air mass flow rate, kg/s

ε_s = sensible effectiveness %

Substituting the NTU value with the equation (23) the final equation (24) for the model was created.

$$\varepsilon = 1 - \exp\left\{\left(\frac{1}{C_r}\right)\left(\frac{UA}{C_{min}}\right)^{-0.22}\left[\exp\left(-C_r \cdot \left(\frac{UA}{C_{min}}\right)^{0.78}\right) - 1\right]\right\}, \% \tag{24}$$

Efficiency, calculated using the equation, was used in ASHARE equations in the simplified model equation (12.13).

2.5.1.2 Energy transfer due to latent heat

In cold climate conditions, as the sensible energy is transferred from the exhaust air stream to supply air stream, the dry bulb temperature of exhaust air drops below dew point temperature, causing formation of water droplets on the walls of the heat exchanger. Condensation increases the sensible effectiveness by increasing the heat transfer rate.

According to AHRAE Handbook (American Society of Heating, Refrigerating and Air-Conditioning Engineers, Inc., 2012), one kilogram of condensed moisture transfers about 2440 kJ to incoming air at room temperature.

To account for condensation effect on the heat exchanger supply air leaving temperature, the equation (25) was adjusted.

$$t_{sal} = t_{sae} - \varepsilon_s \frac{C_{min}}{Q_s \rho_s c_{ps}} (t_{sae} - t_{eae}) + \frac{2440 \cdot cond}{Q_s \rho_s c_{ps}}, ℃ \quad (25)$$

The input used for the model was the same as used for the simplifies and for the detailed models.

2.5.1.3 Steady state parametric study

The parametric study was performed to find out the optimal conditions of the transient simulation, and to find out how changing different parameters affect exhaust air behavior in the heat exchanger. The more detailed the simulation is the longer it takes. At some point the level of detail becomes redundant because the change to results becomes insignificant compared to the time required to run the simulation.

The outdoor and indoor conditions for the base model of the parametric study remained the same as in previous chapters. The focus of the parametric study was to evaluate what effect changing different parameters (grid detail level, UA-value, air flow, indoor temperature) would have to the heat exchanger's efficiency and frost in kilograms.

2.5.2 Transient state detailed model

The "detailed model'' calculations were performed for every hour of the year using measurements from the study "Hygrotermiska Förhållanden I Inomhusluften" (Bagge & Johansson, 2015) and statistical weather conditions in different parts of Sweden. The level of detail was determined by the steady state parametric study.

2.5.3 Frost protection strategies

The estimation of risk of frost was a three-step process. The first step was to find out the water content of exhaust air entering, using the equation (5). The second step was to estimate the water content at saturation of exhaust air leaving, using the equation (4). The final step was to

convert the water content from kg-w/kg-da to kg-w/m^3 (using specific volume equation (6)), of both exhaust air entering and exhaust air leaving at saturation, then to subtract them. If the exhaust air entering humidity content is higher than the exhaust air leaving at saturation humidity content and exhaust air leaving temperature was lower than zero, then subtracting them resulted in a volume of water that froze on the heat exchanger's walls.

By repeating these steps for every hour of the year, the number of hours when condensation occurred during the year, and the total volume of condensation were estimated.

The following strategies were put up to test. They were compared by their total energy use. The total energy use was the energy required to heat the supply air leaving the heat exchanger to predefined supply air temperature – 21℃ and/or to preheat supply air entering the heat exchanger while maintaining heat exchanger frost free.

- Supply air entering 100% bypass was a frost control strategy that prevented frost while maintaining 100% ventilation. It eliminated the amount of cold supply air entering the heat exchanger. Face and bypass frost control started when the supply air temperature dropped below frost threshold value. As supply air temperature reached a frost threshold temperature, bypass dampers would close to bypass the supply air, until the temperature would rise above the threshold value again.
- Preheat frost control was a strategy that prevented frost while maintaining 100% ventilation. The incoming outdoor air was preheated to zero degrees Celsius before entering the heat exchanger. The preheater had to be sized for the coldest outdoor air temperature.
- Combination of bypass and preheating was a strategy that prevented frost while maintaining 100% ventilation, 25%,50% or 75% of the incoming outdoor air was bypassed, while preheating the remaining part of the supply air.

2.6 Tools

Jupyter Notebook
Jupiter Notebook is a web based open-source application that allows to run code interactively in a web browser alongside visualization and mark down text for descriptions.

Python
Python is a open-source, general purpose, object oriented, high level interpreted language with an easy syntax and dynamic semantics. Python supports modules and packages, which encourages program modularity and code reuse. The Python interpreter and the extensive standard library are available in source or binary form without charge for all major platforms and can be freely distributed (Python Software Foundation, 2020).

pandas
pandas provide high-level data structures and functions designed to make working with structured or table data faster, easy and expressive. It provides sophisticated index functionality

to make it easy to reshape, slice and dice, perform aggregations and slice subsets of data (McKinnely, 2018).

NumPy
NumPy, short for Numerical Python, NumPy provides. The data structure, algorithms and library needed to for most scientific applications involving numerical data in Python. For numerical data NumPy arrays are more efficient in storing and manipulating data the other Python built in data structures (McKinnely, 2018).

matplotlib
matokitlib is most popular python library for producing plots and other two-dimension data visualizations. It's designed to produces plot suitable for publications (McLeod, 2019).

PyQt
PyQt is a set of Python bindings for The Qt Company's Qt application framework and runs on all platforms supported by Qt including Windows, macOS, Linux, iOS and Android. The bindings are implemented as a set of Python modules and contain over 1.000 classes (Riverbank Computing Limited, 2020). It was used to create a Graphical User Interface (GUI).

Table 1 Used tools and their versions.

Tool	Source	Version
Jupyter Notebook	https://jupyter.org	6.0.1
Python	http://www.python.org	3.6
Numpy	https://numpy.org/	1.11.3
Pandas	https://pandas.pydata.org/	0.23.4
Matplotlib	https://matplotlib.org/	3.1.1
PyQt	https://www.qt.io/	5

3 Results and analysis

3.1 Outdoor climate conditions

Assuming the sensible efficiency is 80%, and indoor temperature is 21°C, if the outdoor temperature drops below -5°C, the exhaust air will drop below 0°C. See the equation (26). The figure 11 represents the split of hours when temperature in each city was below -5°C, between -5°C and 0°C and above 0°C.

$$t_{outdoor} = \frac{t_{eal} - t_{eae}}{\varepsilon_s \frac{C_{min}}{C_e}} + t_{eae} \quad (26)$$

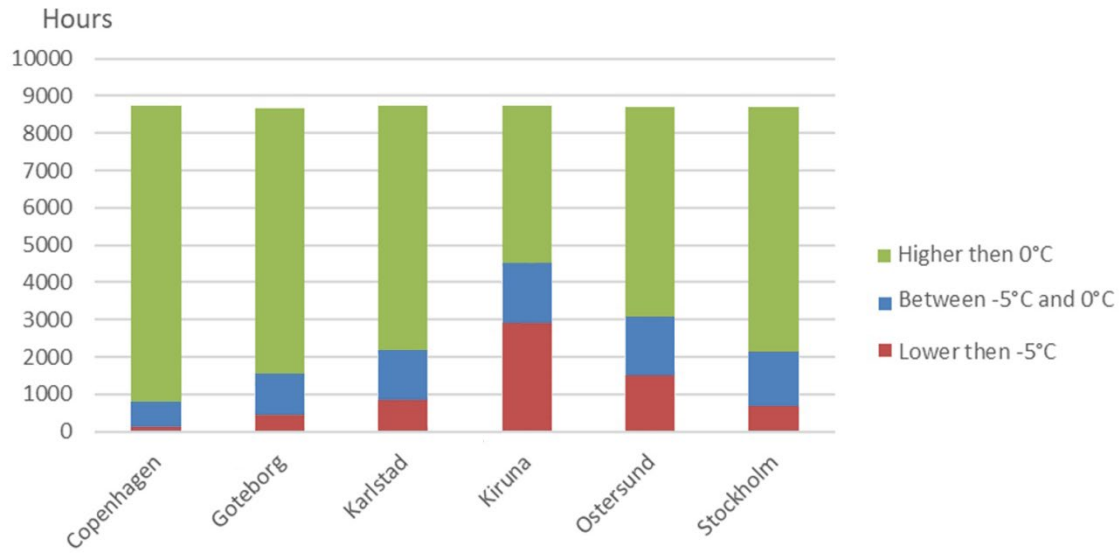

Figure 11 Hour count splinted in 3 temperature groups

Kiruna had the greatest number of hours with risk of frost – 2900 hours in a year when temperature was below -5°C. Copenhagen had the lowest number of hours with a risk of frost- 100 hours in a year.

For the steady state analysis Kiruna's worst conditions from weather file were used. The worst conditions -27°C and RH 80 %.

It does not seem that the risk would be significant in Copenhagen, Gothenburg, Karlstad and Stockholm. The risk is quite high in Kiruna and Ostersund. Since Kiruna had the greatest risk of frost, the steady state calculations were chosen to represent the worst-case scenario that could happen in this city.

3.2 Indoor climate conditions

Total moisture supply (vapor content indoors – vapor content outdoors) was significantly higher in apartments Lg19 and Lg26, they had moisture supply of 33 and 28 kg/m^2/year respectively figure 12.

Figure 12 Total moisture supply in kg per m^2 of apartment area

Violin chart represents hourly total moisture supply in grams per m^2 of apartment area per year for the 10 apartments with highest median value. The width of each,''violin'' represented the frequency of data points in each apartment.

The maximum moisture supply condition was 17g/m^2/h × 75m^2 = 1.3kg/h in apartment Lg17.

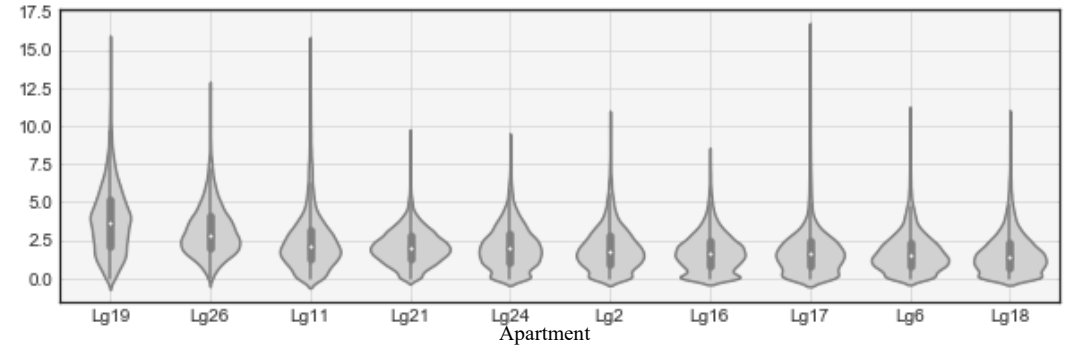

Figure 13 total moisture supply in g per m^2 of apartment area per every hour of the year for the top 10 most risky apartments

The amount of moisture supply per year was unevenly varying from 33 kg/m^2/year to 5kg/m^2/year, which suggested that having one heat exchanger for several apartments could reduce the risk of moisture load per heat exchanger, consequently reducing the risk of frost accumulation.

Even though most of the data points were within the range of 0 to 5 g/m^2, the frost protection system had to be designed to perform well under the peak conditions - 17 g/m^2.

3.3 Steady state simplified simulation

As a basis for simplified dynamic model, steady state calculations were performed on the worst-case scenarios for two kinds of theoretical heat recovery systems - sensible recovery ventilation unit and total energy recovery unit.

3.3.1 Steady state sensible heat recovery ventilation

Outdoor supply air enters sensible heat recovery ventilation unit at -27°C (246.15 K) temperature and at relative humidity of 90%, the supply air flow is approximated to be 0.35 l/s · m^2. The indoor temperature was 21°C (294.15 K) and moisture supply was 1.2 kg-water/h. The energy recovery unit's sensible heat efficiency $\varepsilon_s = 80\%$. The building is assumed to be at sea level and at the atmospheric pressure: ptot = 101.325 kPa. The coefficient's equations (5,6) C1 = -5674.5359, C2 = 6.3925247, C3 = -0.009677843, C4 = 6.22157E-07, C5 = 2.07478E-09, C6 = -9.48402E-13, C7 = 4.1635019 were derived from Hyland-Wexler equations (Hyland & Wexler, 1983b). The amount of frost in the HRV unit under steady state conditions needs to be determined.

Supply air entering stream properties

Supply air flow rate obtained from

Q_{sae} = 74.75m^2· 0.35 l/s · m^2 = 94.185 m^3/h

The saturation pressure of supply air entering stream for temperature -27°C was found from Equation (3) as

$$ln\, p_{ws}sae = \frac{-5674.5359}{246.15} + 6.3925247 + -0.009677843 \cdot 246.15 + 6.22157\text{E} - 07 \cdot 246.15^2 + 2.07478\text{E} - 09 \cdot 246.15^3 + -9.48402\text{E} - 13 \cdot 246.15^4 + 4.1635019 \cdot ln246.15$$

$p_{ws}sa$ = 0.052 kPa

The humidity ratio of supply air entering steam was found from Equation (5) using relative humidity and saturation pressure as

$$Wsae = \frac{0.621945 \cdot 90\% \cdot 0.052\ \text{kPa}}{101.325\ \text{kPa} - 90\% \cdot 0.052\ \text{kPa}} = 0.0003\ \ \text{kg}_\text{w}/\text{kg}_\text{da}$$

Specific volume v of supply air entering stream was found from Equation (6) as

$$v_{sae} = 0.287\,042 \cdot 246.15\ \text{K} \cdot \frac{1 + 1.607\,858 \cdot (0.0003\ \text{kg}_\text{w}/\text{kg}_\text{da})}{101.325\ \text{kPa}} = 0.698\ m^3/kg_{da}$$

Water content in kg per m^3 of dry obtained from

$$W_{sae} = \frac{Wsae}{v_{sae}} = \frac{0.0003\ \mathrm{kg_w/kg_{da}}}{0.698\ m^3/kg_{da}} = 0.0004\ \mathrm{kg_w}/{m^3}_{da}$$

Supply air entering stream mass flow obtained from

$$m_{sae} = \frac{94.185\ \mathrm{m^3/h}}{0.697 m^3/kg_{da}} = 134.710\ kg/h$$

Exhaust air stream properties

Exhaust air entering air flow rate obtained from

Q_{eae} = 74.75m^2· 0.35 l/s · m^2 = 94.185 $m^3{}_{da}$/h

Moister supplied by occupants to one square meter of supply air was obtained from

$$W_{ms} = \frac{\text{Moisture Supply}}{\mathrm{Q_{eae}}} = \frac{1.2\ \mathrm{kg_w}}{94.185\ \mathrm{m^3}_{da}/\mathrm{h}} = 0.0126\ \mathrm{kg_w}/\mathrm{m^3}_{da}$$

Specific volume of dray air was found from Equation (6) as

$$v_{sae} = 0.287\ 042 \cdot 294.15\ \mathrm{K} \cdot \frac{1 + 1.607\ 858 \cdot (0\ \mathrm{kg_w/\ kg_{da}})}{101.325\ \mathrm{kPa}} = 0.833\ m^3/kg_{da}$$

The humidity ratio of exhaust air entering stream was obtained from

$$\begin{aligned}\mathrm{W_{eae}} &= (W_{ms} + W_{sae}) \cdot \rho_{da} \\ &= (0.0126\ \mathrm{kg_w}/\mathrm{m^3}_{da} + 0.0004\ \mathrm{kg_w}/\mathrm{m^3}_{da}) \cdot 0.833\ \mathrm{m^3}_{da}/\mathrm{kg}_{da} \\ &= 0.0108\ \mathrm{kg_w}/\mathrm{kg}_{da}\end{aligned}$$

Exhaust air entering stream mass flow obtained from

$$m_{eae} = \frac{Q_{eae}}{v_{sae}} = \frac{94.185}{0.833} = 113.067\ kg/h$$

Exhaust air leaving temperature was found from Equation (13) as

$$t_{sal} = 21 - 80\% \cdot \frac{113.067\ kg/h \cdot (1.006\ kJ/kg \cdot K)}{113.067\ kg/h \cdot (1.006\ kJ/kg \cdot K)} \cdot abs(-27°C - 21°C) = -17.4°C$$

The saturation pressure of exhaust air leaving stream for temperature -17.4℃ was found from Equation (3) as

$$ln\, p_{ws}sa = \frac{-5674.5359}{255.75\ \text{K}} + 6.3925247 + -0.009677843 \cdot (255.75\ \text{K}) + 6.22157\text{E} - 07 \cdot (255.75\ \text{K})^2 + 2.07478\text{E} - 09 \cdot (255.75\ \text{K})^3 + -9.48402\text{E} - 13 \cdot 255.75^4 + 4.1635019 \cdot \ln(255.75\ \text{K}) = 0.123\ \text{kPa}$$

The humidity ratio at saturation of exhaust air leaving was found from Equation (5) as

$$W_{eal\ sat.} = \frac{0.621945 \cdot 0.123\ \text{kPa}}{101.325\ \text{kPa} - 0.123\ \text{kPa}} = 0.001\ kg_w/kg_{da}$$

The amount of water that was condensed during the heat transfer process was obtain from

$$\text{Condensation} = (\text{W}_{\text{eae}} - W_{eal\ sat.} \cdot \text{m}_{\text{eae}} = (0.011\ kg_w/kg_{da} - 0.001\ kg_w/kg_{da}) \cdot 113.067\ kg/h = 1.131\ \text{kg}_w/h$$

Since the temperature was lower then 0℃ the condensation was equal to frost.

The energy recovered was found from Equation (9) as

$$q_s = 113.406 \cdot (1.006\ kJ/kg \cdot K) \cdot (21°C - (-17.4°C)) = 4\,354.790\ kJ = 120.966\ kWh$$

3.3.2 Steady state total energy recovery ventilation

Initial temperatures and constants were assumed to be the same as in the section 3.3.1 “Steady state sensible heat recovery ventilation”. Outdoor supply air enters latent heat recovery ventilation unit with $m_{sae} = 135.519\ kg/h$ mas flow and $W_{sae} = 0.0003\ kg_w/kg_{da}$ humidity ratio. Indoor supply air enters heat recovery ventilation unit with $m_{eae} = 113.406\ kg/h$ and $W_{eae} = 0.011\ kg_w/kg_{da}$ humidity ratio. Maximum possible water content of the exhaust air in the ERV was estimated in the section 3.3.1 $W_{ael_{sat.}} = 0.001\ kg_w/kg_{da}$ .The latent efficiency of the unit is assumed to be $\varepsilon_L = 50\%$. The amount of frost in the HRV unit under steady state conditions need to be determined.

The humidity ratio of supply air entering steam was estimated from Equation (5) using relative humidity and saturation pressure as

$$w_{sal} = 0.011 - 50\% \cdot \frac{113.406}{135.519}(0.011 - 0.0003) = 0.005\ kg_w/kg_{da}$$

The humidity ratio of supply air leaving steam was found from Equation (5) using relative humidity and saturation pressure as

$$w_{eal} = 0.0003 + 50\% \cdot \frac{113.406}{135.519}(0.011 - 0.0003) = 0.007\ kg_w/kg_{da}$$

The amount of water that was condensed during the heat transfer process was obtain from

$$w_{eal} = 0.001 < 0.007 = 0.001\ kg_w/kg_{da}$$

$$cond = (0.007 - 0.001) \cdot 136.33 = 0.783\ kg_w$$

The ERV had a significantly lower amount of theoretical frost. almost a half of HRV - 0.783kg-w 1.583 kg-w. this would suggest that having an ERV would be more beneficial compared to HRV in colder climates due to moisture transfer to supply air stream.

3.3.3 Simulating different heat exchangers arrangements

Table, 2 represents the difference that having different number of heat exchangers in a building can make during the hours of a year when risk of frost can occur. When the building had multiple heat exchangers, each unit tended to have different number of hours of risk of frost. The table represents the average number of hours of risk of frost, in the specific scenarios.

Table 2 Count of risk of frost hours per by city and by number of units in the apartment building for sensible heat exchange

Air flow	Tin	Units	Cph	Froson	Goteborg	Karlstad	Kiruna	Sthlm
3384 m³/h	21°C	1	133 h	925 h	244 h	545 h	1652 h	444 h
1692 m³/h	21°C	2	134 h	915 h	248 h	543 h	1645 h	442 h
846 m³/h	21°C	4	136 h	915 h	254 h	572 h	1619 h	438 h
565 m³/h	21°C	9	145 h	881 h	274 h	554 h	1620 h	443 h
94 m³/h	21°C	36	137 h	864 h	265 h	526 h	1518 h	404 h

The table 3 represents the amount of frost formation in kilograms that could theoretically occur in plate heat exchangers, without any strategy of protection from frost applied.

Table 3 Amount of frost formation per by city and by number of units in the apartment building for sensible heat exchange

Air flow	Tin	Units	Cph	Froson	Gtb	Karlstad	Kiruna	Sthlm
3384 m³/h	21°C	1	224 kg	1836 kg	384 kg	1178 kg	3605 kg	836 kg
1692 m³/h	21°C	2	237 kg	1863 kg	410 kg	1198 kg	3653 kg	866 kg
846 m³/h	21°C	4	252 kg	1976 kg	487 kg	1320 kg	3770 kg	901 kg
565 m³/h	21°C	9	336 kg	2317 kg	618 kg	1406 kg	4211 kg	1015 kg
94 m³/h	21°C	36	515 kg	3242 kg	1002 kg	2084 kg	5642 kg	1510 kg

The table 4 represents the difference that having different number of enthalpy wheels in a building can make during the hours of a year when risk of frost can occur. When the building had multiple enthalpy wheels, each unit tended to have different number hours of risk of frost. The table represents the average number of hours of risk of frost, in the specific scenarios.

Table 4 Count of risk of frost hours per by city and by number of units in the apartment building for enthalpy well

Air flow	Tin	Units	Cph	Froson	Gtb	Karlstad	Kiruna	Sthlm
3384 m^3/h	21°C	1	107h	4h	35h	350h	4h	107h
1692 m^3/h	21°C	2	108h	10h	38h	361h	5h	108h
846 m^3/h	21°C	4	110h	8h	46h	369h	16h	110h
565 m^3/h	21°C	9	130h	16h	69h	397h	28h	130h
94 m^3/h	21°C	36	208h	50h	126h	485h	78h	208h

The table 5 represents the amount of frost formation in kilograms that could theoretically occur in enthalpy wheels, without any strategy of protection from frost applied.

Table 5 Amount of frost formation per by city and by number of units in the apartment building for enthalpy wheel

Air flow	Tin	Units	Cph	Froson	Gtb	Karlstad	Kiruna	Sthlm
3384 m^3/h	21°C	1	0 kg	65 kg	1 kg	25 kg	280 kg	2 kg
1692 m^3/h	21°C	2	0 kg	68 kg	2 kg	27 kg	314 kg	2 kg
846 m^3/h	21°C	4	0 kg	76 kg	4 kg	31 kg	335 kg	7 kg
565 m^3/h	21°C	9	2 kg	119 kg	11 kg	71 kg	410 kg	19 kg
94 m^3/h	21°C	36	43 kg	401 kg	103 kg	251 kg	885 kg	156 kg

After the simulation with the simplified model, the results showed that the number and the arrangements of the plate heat exchangers in the building did not make a significant difference regarding hours the risk of freezing occurred. The biggest difference occurred between having 1 unit for the whole building and having one unit for each apartment – 36 units in total. However, the difference in theoretical amounts of frost-formation was significant. The fewer units were used, the lower the theoretical frost-load. Even though the number of hours of risk did not change significantly, reducing the number of heat exchangers could lead to lower load of frost formation and less energy-requiring frost protection strategies.

On the other hand, in the building with enthalpy wheels both the risk of frost formation and the theoretical frost-load reduced significantly due to reduction of the number of enthalpy wheel units in the building, making reducing the number of enthalpy wheel units a valid strategy to reduce the risk of frost.

3.4 Detailed heat exchanger simulation

3.4.1 Steady state detailed model

3.4.1.1 Energy transfer due to dry bulb temperature difference

The main difference between the simplified model and the detailed model was that instead of dimensionless efficiency, used in the simplified model, the detailed model uses UA value- 0.15. Table 6.

Table 6 Input for simulation

UA - Value	0.15
Air Supply (l/s)	0.35
Atmospheric Pressure (kPa)	101.325
Indoor Temperature (°C)	21
Outdoor Temperature (°C)	-27
Outdoors RH (%)	90%
Moisture Supply (g/m2/h)	16
Grid detail level	100x100

Based on the steady state conditions and the UA value, the efficiency was calculated to be 80%, which is comparable to the simplified steady state input used in previous chapters.

$$\varepsilon = 1 - \exp\left\{\left(\frac{1}{C_r}\right)\cdot\left(\frac{UA}{C_{min}}\right)^{-0.22}\cdot\left[\exp\left(-C_r\cdot\left(\frac{UA}{C_{min}}\right)^{0.78}\right)-1\right]\right\},\% \quad (27)$$

$$C_r = \frac{(mc_p)_{min}}{(mc_p)_{max}} \quad (28)$$

The detailed simulation results were represented in a heatmap of exhaust air, revealing the temperature distribution and the cold corner of the heat exchanger figure 14.

Frost appears in more than ≈50% of the HE's cross section, condensation appears in ≈20% figure 15.

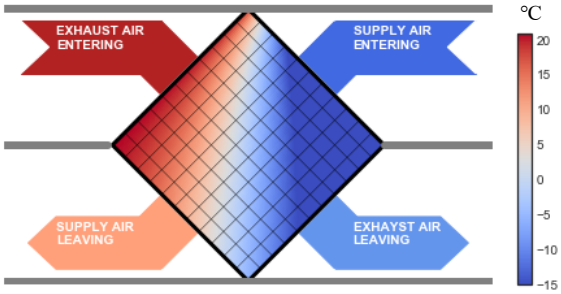

Figure 14 Heat map of exhaust air temperature distribution.

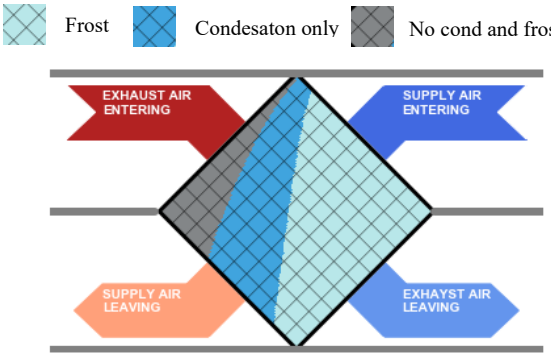

Figure 15 Heat map representing the distribution of frost and condensation within heat exchanger exhaust air channels.

The results and comparison of the simplified and the detailed models were represented in table 7.

Table 7 Simulation results in comparison with simplified model

Measure	**Simplified**	**Detailed**
Condesation	**0 kg**	**0.7835 kg**
Frost	**1.123 kg**	**0.3219 kg**
Average Supply Air Leaving Temp	4.64°C	4.57°C
Average Exhaust air Leaving Temp	-17.46°C	-17.01°C
Energy Recovered	1.209 kWh	1.191 kWh
Efficiency	80%	80%

The detailed model showed that frost and condensation appeared at the same time in different areas of the cross section of the HE. The main difference between the simplified model and the detailed model was that the simplified model, differently than the detailed model, did not separate areas of frost and condensation, assuming that they appear across the whole HE, making the simplified model insufficient for these types of analyses.

Other than the difference between frost and condensation, other results did not differ significantly.

3.4.1.2 Energy transfer due to latent heat

Frost and condensation areas in the cross section of the HE was ≈30% and ≈30% respectively. Figure 16 and figure 17

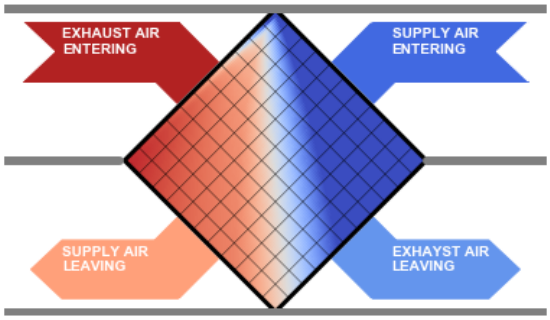

Figure 16 Heat map of exhaust air temperature distribution.

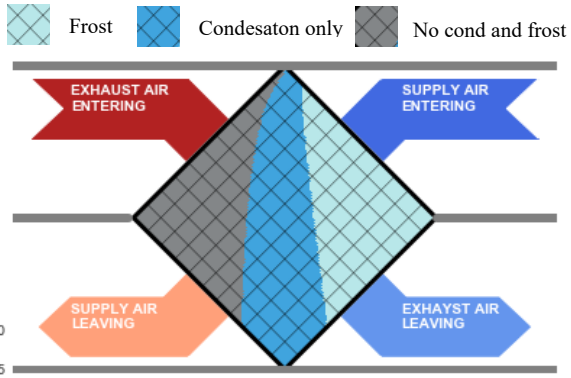

Figure 17 Heat map representing the distribution of frost and condensation within heat exchanger exhaust air channels.

The final results were presented in the table 7 together with the simplified and the detailed model's results.

Table 8 Simulation results in comparison with simplified model and detail model without condensation effect

Measure	Simplified	Detailed	Cond effect
Condesation	0 kg	0.7835 kg	0.7131 kg
Frost	1.123 kg	0.3219 kg	0.2175 kg
Average Supply Air Leaving Temp	4.64°C	4.57°C	15.03°C
Average Exhaust air Leaving Temp	-17.46°C	-17.01°C	-17.01°C
Energy Recovered	1.209 kWh	1.191 kWh	1.585 kWh
Efficiency	80%	80%	106%

Frost and condensation areas in the cross section of the HE shifted from ≈50% to ≈30% and from ≈20% to ≈30% respectively, due to more drastic temperature.

With condensation taken into account, energy recovery increased due to the increase of efficiency, which reached more than 100%, due to latent energy transfer. Condensation and frost decreased by 9% and 32% respectively, due to the increase of supply air leaving temperature.

The final model, which included condensation effect, was more accurate compared to the simplified and the detailed models. The results differed significantly, making the analysis of such a type more reliable.

3.4.2 Steady state parametric study

The results from the parametric study of the grid detail level were plotted in figure 18. The line chart and the bar chart, which shared the x axes, represented exhaust air leaving temperature and frost in kilograms, respectively.

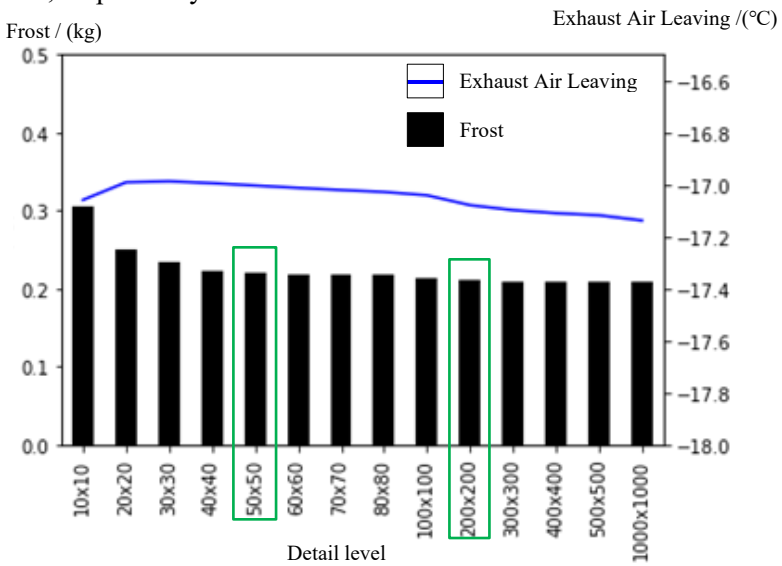

Figure 18 Relationship between grid detail level and change of exhaust air temperature and frost volume in kg.

The results from the parametric study of UA-value of the heat exchanged were plotted in figure 19. The line chart and the bar chart, which shared the x axes, represented exhaust air leaving temperature and frost in kilograms, respectively.

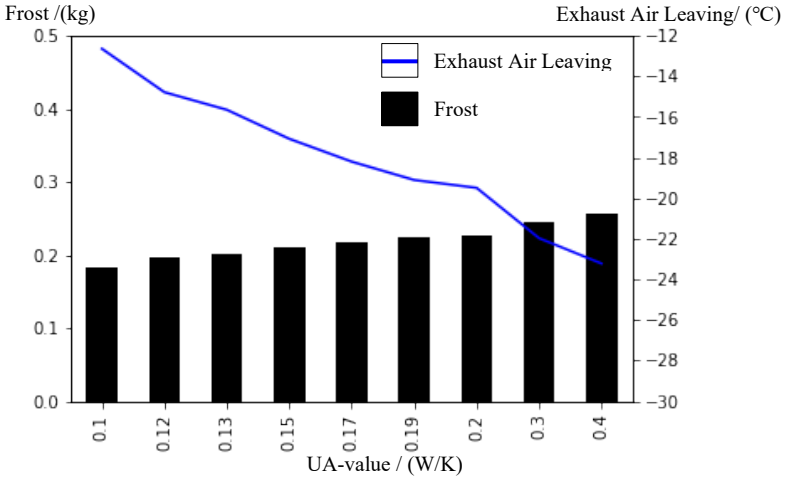

Figure 19 Relationship between UA-value and the change of the exhaust air temperature and frost volume in kg.

The results from the parametric study of exhaust air entering were plotted in figure 20. The line chart and the bar chart, which shared the x axes, represented exhaust air leaving temperature and frost in kilograms, respectively.

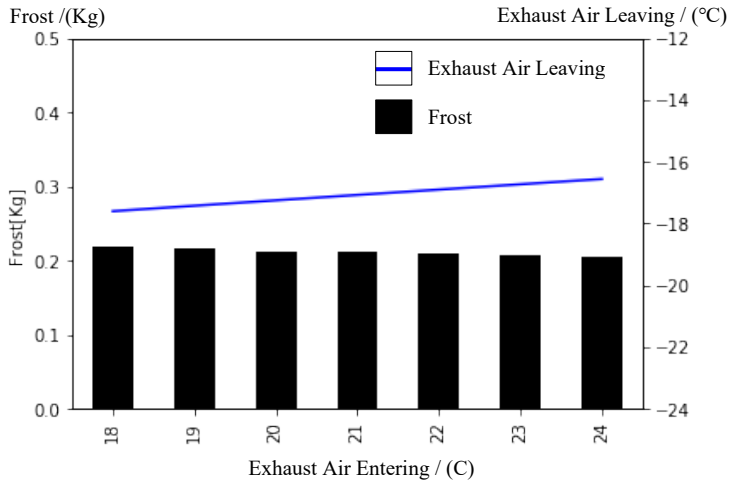

Figure 20 Relationship between exhaust air entering and the change of the exhaust air temperature and frost volume in kg.

The results from the parametric study of air flow were plotted in figure 21. The line chart and the stacked bar chart, which shared the x axes, represented heat exchanger efficiency and frost/condensation in kilograms, respectively.

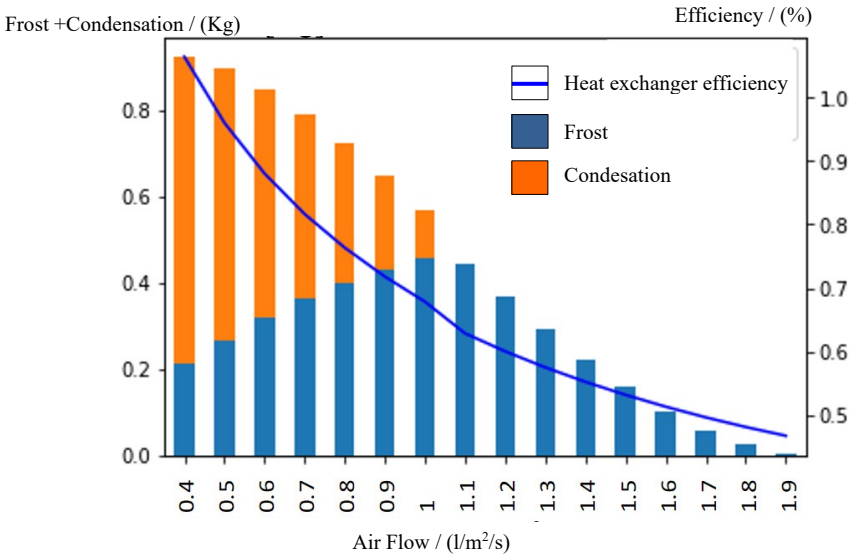

Figure 21 Effect of different air flows on volume of condensation/ frost and heat exchanger efficiency

When the grid detail was at its minimum – 10x10, amount of frost was at it's highest. Increasing the grid detail resulted in a drop of the amount of frost without lowering exhaust air leaving temperature significantly. When the grid detail reached 40x40, the drop of the amount of frost stabilized until the grid detail was increased to 100x100. After that an insignificantly small effect to frost formation was noticed.

Changing UA-value effected the efficiency of the heat exchanger. Increasing it resulted in a higher risk of frost formation and lower exhaust air temperature. At the UA-value of 0.19 the efficiency was around 80%. This UA-value has been selected as the size of the heat exchanger of this study.

The amount of frost formation was not significantly affected by the changes in temperature of exhaust air entering.

When increasing the air flow up to 1.1, the amount of frost also increased while the amount of condensation decreased. When the air flow became 1.1 and higher, the amount of frost started to decrease, and condensation disappeared. Efficiency was at its highest when the air flow was 0.35, increasing the airflow decreased efficiency.

3.4.3 Transient simplified sensible heat recovery ventilation model

Every cities' boxplot in the figure 22 represents 36 data points, one data point represents one apartment, one point represent total amount of hours when there is risk for frost to be formed.

Box plots show the five-number summary of a set of data: including the minimum score, first (lower) quartile, median, third (upper) quartile, outliers (circle) and maximum score (McLeod, 2019).

The heat recovery system had the lowest risk of frost formation when it was placed in Copenhagen, having the maximum of 490 hours of frost per year. The highest risk of frost formation was in Kiruna with the maximum of 3650 hours of frost per year.

Majority of data points from Copenhagen, Gothenburg and Karlstad were below 500 hours of frost per year, putting them in the same category.

There are few outliers in every city with a higher risk of frost formation than the majority of apartments.

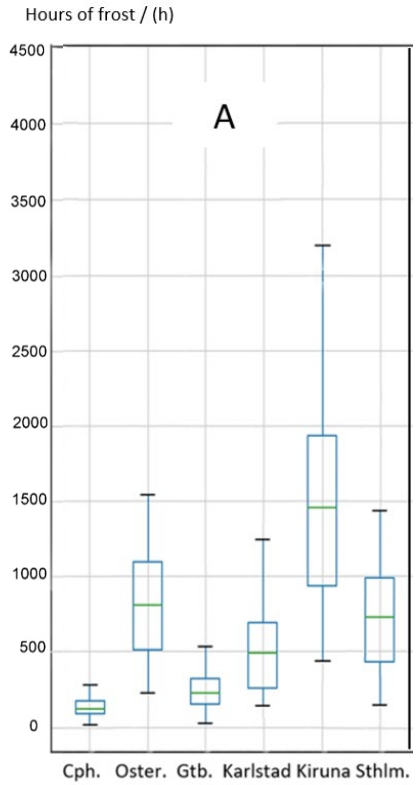

Figure 22 Hours at risk of frost formation, grouped by the city, estimated using transient simplified sensible heat recovery ventilation model

Even though Copenhagen and Gothenburg had relatively warm weather conditions HRS still had a risk of frost formation.

Even though the highest instances were solitary and much higher than the majority of data points, they must be covered by the frost protection systems.

3.4.4 Transient simplified total heat recovery ventilation model

Every cities' boxplot in the figure 23 represents 36 data points, one data point represents one apartment, one point represent total amount of hours when there is risk for frost to be formed. The energy recovery system of the research paper had the lowest risk of frost formation when it was placed in Copenhagen, having the maximum of 260 hours of frost per year, with many data points at zero hours of frost per year. The highest risk of frost formation was in Kiruna with the maximum of 2400 hours of frost per year.

Majority of data points from Copenhagen, Gothenburg, Froson, Karlstad and Stockholm were between zero and 250 hours of frost per year, putting them in the same category.

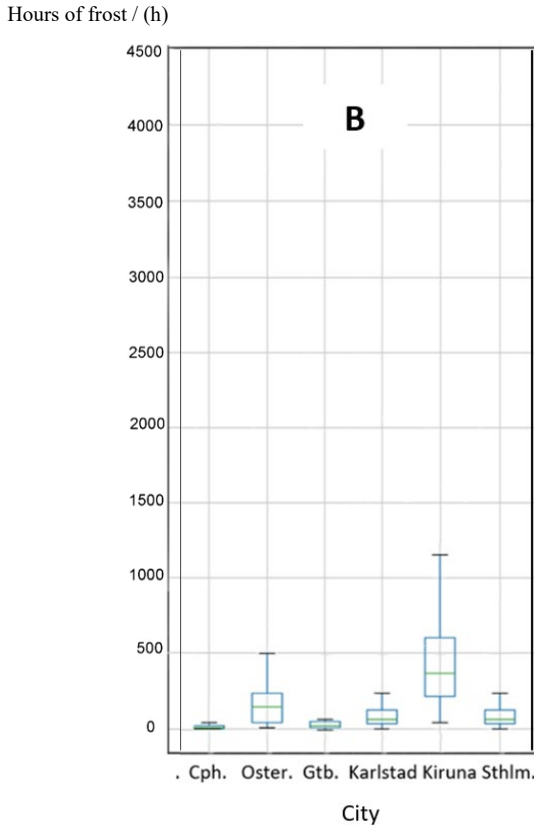

Figure 23 Hours at risk of frost formation, grouped by the city, estimated using transient simplified total heat recovery ventilation model

Risk of frost formation became significantly lower in every city when HRV was changed into ERV. Kiruna remained the city with the highest risk of frost formation, however. with ERV instead of HRV it reached the same level of frost formation risk as Copenhagen and Gothenburg (the cities with the lowest risk with HRV) did with HRV instead of ERV.

3.4.5 Transient detailed sensible heat recovery ventilation model

Every cities' boxplot in the figure 24 represents 36 data points, one data point represents one apartment. The heat recovery system of the research paper had the lowest risk of frost formation when it was placed in Copenhagen, having the maximum of 600 hours of frost per year. The highest risk of frost formation was in Kiruna with the maximum of 4850 hours of frost per year.

Copenhagen is the only city with majority of data points below 500.

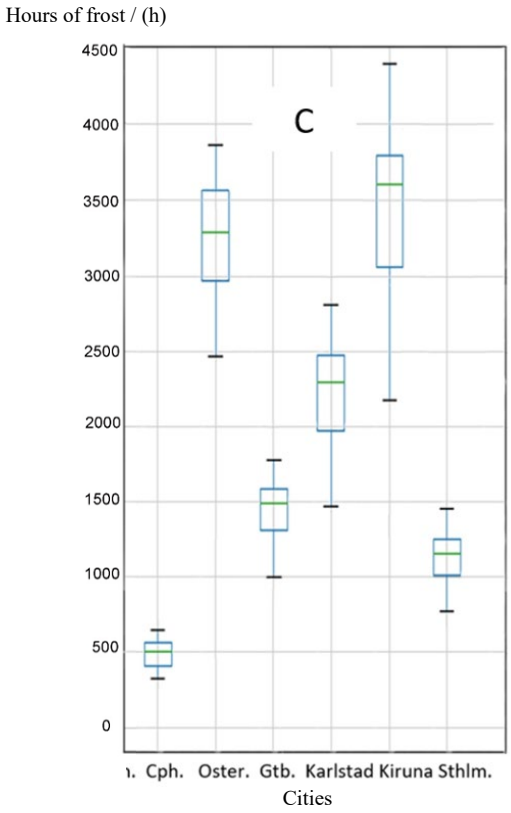

Figure 24 Hours at risk of frost formation, grouped by the city, estimated using transient detailed sensible heat recovery ventilation model

The detailed model uncovered many hours of risk of frost formation that were not included in the simplified model. As a result, there was a more distinct difference between the cities and much higher risk of frost formation in every city overall. The outliers became much closer to the majority of data points, compared to the simplified model.

3.4.6 Frost protection strategies

Each bar represents a different strategy that was tested using the calculation model and simulating Kiruna weather conditions. The system without a bypass damper performed the best in regard to total energy use (*Energy for heating + Energy to preheat incoming air*).

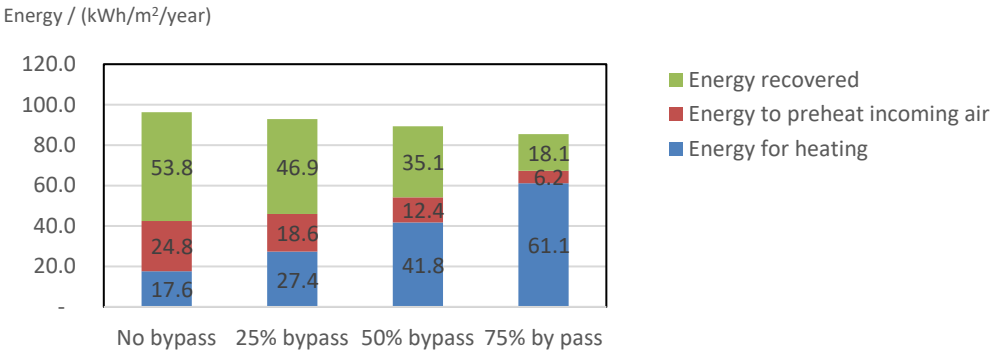

Figure 25 Energy use and saving by different frost protection strategy. 100% by-pass is not included in the picture as it would only increase the energy use needed to supply/buy to the ventilation system.

Bypass strategies, while effective at eliminating the risk of frost in heat recovery unit, were not performing as well from energy perspective. The red and blue parts in Figure 25, representing the energy needed to buy/supply to the air, should be small from an energy perspective. The more air was by-passed, the fewer the opportunities to recover energy from exhaust air, leading to lower supply air temperatures, thus higher energy need for heating a living space.

4 Conclusion

The first objective to analyze selected indoor and outdoor conditions has been reached. The part of the analysis, that can be found in the sections 3.1 led to conclusion that the risk for the frost in the heat exchanger was highest in Kiruna and Ostersund due low outdoor air temperatures during the winter. The Other part of the analysis that can be found in the section 3.2 led to the conclusion that the moisture supply was unevenly occurring within building's apartments, suggesting that the moisture load in a heat exchanger could be reduced by having less, but bigger heat exchangers that gather exhaust air streams from several apartments at once.

The second objective, to propose a reasonable simulation model, has been reached. In the process, which is described in sections 3.3 to 3.4.1, several increasingly detailed and sophisticated frost simulation models were built: the simplified simulation models, the detailed model that enables to analyze frost accumulation across cross section area of square shaped plate heat exchangers, and, in the final version of the model, the additional calculations were added to include the condensation effect. Including the condensation effect in the detailed model made a big difference to the results. The final model was proven to be worthy to use in further investigations, due to results that more accurately represent real word conditions.

The third objective, to discuss and investigate risk of frost formation and different frost protection strategies, was reached. The final detailed model, which was discussed in the section 3.4.1.2, resulted in decreasing the amount of condensation and frost, compared to the simplified model. This happened because the detailed model revealed that frost occurs not uniformly across the cross section but starting in the cold corner and where exhaust air and supply air cross each other. Running the transient simulation models, that are discussed in the sections 3.4.3 to 3.4.5, showed that even though Copenhagen and Gothenburg had relatively warm weather conditions, heat recovery systems still had a risk of frost formation. Risk of frost formation became significantly lower in every city when heat recovery ventilation was changed into energy recovery ventilation. Even though heat recovery ventilation was simulated only with the simplified model, it is safe to assume that it will still be effective in reality. Although bypass strategies, that were discussed in the section 3.4.6, were effective at eliminating the risk of frost in heat recovery unit, they were not as efficient from energy perspective. The more air by-passes the cross-flow plate heat exchanger, the fewer opportunities there are to recover energy from exhaust air, which leads to lower supply air temperatures and higher energy need for heating a living space.

Due to time and limitation, the study could not be expanded any further. Analyze different frost protection strategies, design a detailed model for enthalpy wheel, design different shapes of cross flow heat exchanger, building even more sophisticated models are topics that are possible.

5 References

Python Software Foundation. (den 1 12 2020). *https://www.python.org/doc/essays/blurb/*. Hämtat från Python Essays: https://www.python.org/doc/essays/blurb/

Abel, E., & Elmrofth, A. (2007). *Buildings and energy - a systematic approach.* Stockholm: Formas.

American Society of Heating, Refrigerating and Air-Conditioning Engineers. (2009). *ASHRAE Handbook - Fundamentals.* Atlanta: American Society of Heating, Refrigerating and Air-Conditioning Engineers, Inc. (ASHRAE).

American Society of Heating, Refrigerating and Air-Conditioning Engineers, Inc. (2012). *Heating, Ventilating,and Air-Conditioning SYSTEMS AND EQUIPMENT.* Atlanta: American Society of Heating, Refrigerating and Air-Conditioning Engineers, Inc. (ASHRAE).

Bagge, H., & Johansson, D. (2015). *Hygrotermiska Förhållanden I Inomhusluften.* Helsinborg: Lunds University.

Dewitt, D. P., Incropera, F. P., Bergman, T. L., & Lavine, A. S. (2007). *Fundamentals of Heat and Mass Transfer.* Los Angeles: John Wiley & Sons.

eea.europa.eu. (den 1 January 2015). *final-energy-consumption-by-sector*. Hämtat från eea.europa.eu: https://www.eea.europa.eu/data-and-maps/indicators/final-energy-consumption-by-sector-5/assessment

Fernando Pérez, B. G. (October 2020). *Jupyter Notebook*. Hämtat från jupyter: https://jupyter.org/

Hyland, R., & Wexler, A. (1983b). Frmulation of the thermodinamic properties of the saturated phase of H20 from 173.15 K to 473.15 K. i R. Hyland, & A. Wexler, *ASHRAE transactions 89(2A)* (ss. 500-219). Atlanta: The American Society of Heating, Refrigerating and Air-Conditioning Engineers.

INCROPERA, F. P., DAVID , D. P., THEODORE , B. L., & ADRIENNE , L. S. (2007). *Fundamentals of Heat and Mass Transfer.* Los Angeles: John Wiley & Sons, Inc.

INCROPERA, F. P., DEWITT, D. P., BERGMAN, T. L., & LAVINE, A. S. (2007). *Fundamentals of heat and mass transfer.* Manhattan : JOHN WILEY & SONS.

McKinnely, W. (2018). *Python for Data Analysis.* Milton Keinsas: O'Reily Media, Inc.

McLeod, S. (2019). *What does a box plot tell you?* Hämtat från simplypsychology: https://www.simplypsychology.org/boxplots.html#:~:text=A%20box%20plot%20(also%20known,(or%20percentiles)%20and%20averages.

National Renewable Energy Laboratory. (den 1 12 2020). *weather*. Hämtat från energyplus: https://energyplus.net/weather

Rafatinasr, M. (2016). *FROSTING IN MEMBRANE ENERGY EXCHANGERS.* Saskatoon: University of Saskatchewan.

Riverbank Computing Limited. (den 1 12 2020). *pyqt*. Hämtat från riverbankcomputing: https://riverbankcomputing.com/software/pyqt

Jupiter Notebook. version 6.0.1. Available at https://jupyter.org. was used as an interpreter and representation tool.
Python Software Foundation. Python Language Reference. version 3.6. Available at http://www.python.org. was a programing language used to script the calculations into the modules.
Numpy. version 1.11.3 and Pandas. version 0.23.4. Available at https://numpy.org/ and https://pandas.pydata.org/ respectably. were python libraries used for most of the calculations and iterations.
Matplotlib version 3.1.1. Available at https://matplotlib.org/. was a library used to create graphs and plots to visually represent the data.
PyQt version 5. Available at https://www.qt.io/ libraries were used to create a Graphical User Interface (GUI).

LUND UNIVERSITY

Dept of Building and Environmental Technology: Divisions of Energy & Building Design, Building Physics and Building Services